FDM analysis for MHD flow of a non-Newtonian fluid for blood flow in stenosed arteries [†]

D. S. Sankar[1] and Usik Lee[2,*]

[1]*School of Mathematical Sciences, Universiti Sains Malaysia, 11800 Penang, Malaysia*
[2]*Department of Mechanical Engineering, Inha University, 253,Yonghyun-Dong, Nam-Gu, Incheon 402-751, Korea*

Abstract

A computational model is developed to analyze the effects of magnetic field in a pulsatile flow of blood through narrow arteries with mild stenosis, treating blood as Casson fluid model. Finite difference method is employed to solve the simplified nonlinear partial differential equation and an explicit finite difference scheme is obtained for velocity and subsequently the finite difference formula for the flow rate, skin friction and longitudinal impedance are also derived. The effects of various parameters associated with this flow problem such as stenosis height, yield stress, magnetic field and amplitude of the pressure gradient on the physiologically important flow quantities namely velocity distribution, flow rate, skin friction and longitudinal impedance to flow are analyzed by plotting the graphs for the variation of these flow quantities for different values of the aforesaid parameters. It is found that the velocity and flow rate decrease with the increase of the Hartmann number and the reverse behavior is noticed for the wall shear stress and longitudinal impedance of the flow. It is noted that flow rate increases and skin friction decreases with the increase of the pressure gradient. It is also observed that the skin friction and longitudinal impedance increase with the increase of the amplitude parameter of the artery radius. It is also found that the skin friction and longitudinal impedance increases with the increase of the stenosis depth. It is recorded that the estimates of the increase in the skin friction and longitudinal impedance to flow increase considerably with the increase of the Hartmann number.

Keywords: Pulsatile blood flow; Casson fluid model; Stenosed artery; Magnetic field; Finite difference method

---

1. Introduction

Among the various cardiovascular diseases, arteriosclerosis/stenosis is a major one which affects the flow of blood in the arteries (causes total blockage in the artery in severe cases) and leads to serious circulatory disorders [1]. Stenoses are formed by the accumulation of fats/ lipids on the inner wall of the arteries [2]. Stenoses developed in the arteries pertaining to brain can cause cerebral strokes and the one developed in the coronary arteries can cause myocardial infarction which leads to heart failure [3]. Several researchers pointed out that the fluid dynamical properties of blood flow through non-uniform cross-section of the arteries plays vital role in the basic understanding and treatment of many cardiovascular diseases [4-6]. Thus, the study of blood flow through stenosed arteries is important.

Extensive research on the dynamics of biological fluids in the presence of magnetic field with applications to the medical field was carried out by several researchers [7-10]. It is well accepted that the biological systems in general are greatly affected by the presence of external magnetic field [11]. Some applications of magnetic devices are cell separation, reduction of bleeding during surgeries and provocation of occlusion of the feeding vessels of cancer tumors [12, 13]. Vardayan [13] reported that a uniform transverse magnetic field alters the flow rate of blood when it flows through arteries of circular cross-section. Bhargava et al. [14] pronounced that magnetic field can be used as a flow control mechanism in medical applications. Hence, it is useful to study the blood flow in arteries in the presence of magnetic field.

Several attempts were made to analyze the blood flow in stenosed arteries in the presence of magnetic field [15-19]. Blood behaves like a Newtonian fluid when it flows through larger arteries at high shear rates, whereas, it exhibits non-Newtonian character when it flows through narrow arteries at low shear rates [20-22]. As blood flow through narrow arteries is highly pulsatile, several researchers analyzed the pulsatile flow of blood in the presence of magnetic field, treating it as a non-Newtonian fluid [10, 23-25]. The pulsatile flow of Casson fluid for blood in stenosed arteries in the presence of magnetic field was not investigated so far using computational methods.

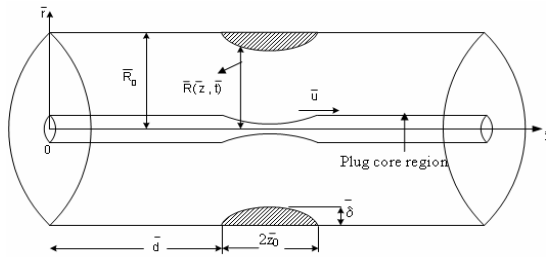Casson fluid model is non-Newtonian fluid with yield stress

---

Fig. 1. Geometry of segment of an artery with stenosis.

which has significant applications in biomechanics [26]. Also, it is a shear thinning fluid, which has an infinite viscosity at a zero rate of shear. Casson [27] investigated the validity of this fluid model in studies pertaining to the flow characteristics of blood and reported that at low shear rates, the yield stress for blood is nonzero. Scott Blair [28] and Copley [29] reported that the parameters of the Casson fluid (viscosity, yield stress and power law) are adequate for the representation of simple shear flow of blood. Merrill et al. [30] spelled out that Casson fluid model holds satisfactorily for blood flowing in tubes of diameter $130 - 1300$ μm. Charm and Kurland [31] pointed out in their experimental findings that the Casson fluid model could be the best representative of blood and that it could be applied to human blood. Further, Scott Blair and Spanner [32] mentioned that blood behaves like a Casson fluid at moderate shear rate flows. Hence, it is appropriate to model blood as Casson fluid when it flows through narrow arteries at moderate shear rates. Hence, in this study, the effect of magnetic field in the pulsatile flow of blood through narrow arteries with axisymmetric mild stenosis is investigated, treating blood as Casson fluid model.

2. Mathematical formulation

2.1 Flow field geometry and governing equations

Since blood exhibits remarkable non-Newtonian character when it flow through narrow arteries at low shear rates, it is modeled as Casson fluid model (non-Newtonian fluid). Since Casson fluid is a non-Newtonian fluid with yield stress, the flow region is divided into two parts: (i) plug flow region and (ii) non-plug flow region. Cylindrical polar coordinate system $(\bar{r}, \bar{\psi}, \bar{z})$ has been used to analyze the flow situation, where $\bar{r}$ and $\bar{z}$ are the radial and axial directions respectively and $\bar{\psi}$ is the azimuthal angle. The geometry of the segment of the arterial with time dependent mild stenosis as shown in Fig. 1. [10, 21] is mathematically represented by

$$\bar{R}(\bar{z},\bar{t}) = \begin{cases} \left[\bar{R}_0 - \dfrac{\bar{\delta}}{2}\left(1+\cos\left[\pi(\bar{z}-\bar{z}_1)/\bar{z}_0\right]\right) \right] a(\bar{t}) & \text{if } \bar{d} \leq \bar{z} \leq \bar{d}+2\bar{z}_0 \\ \bar{R}_0\, a(\bar{t}) & \text{in the non-stenotic region} \end{cases}$$

(1)

where $\bar{R}(\bar{z},\bar{t})$ is the radius of the arterial segment in the constricted region, $\bar{R}_0$ is the radius of the artery in the normal

region, $\bar{\delta}$ is the maximum projection of the stenosis, $\bar{z}_0$ is the semi-length of the stenosis, $\bar{z}_1$ is the centre of the stenosis.

The time-dependent parameter $a(\bar{t})$ is defined by

$$a(\bar{t}) = 1 - k\cos(\bar{\omega}\bar{t} - \phi)$$

(2)

where k is the amplitude parameter, ϕ is the phase angle, $\bar{\omega} = 2\pi\bar{f}$ with $\bar{f}$ being the heart pulse frequency. It is to be noted that Eq. (1) is formulated suitably in such a way that at the end points of the stenosis ($\bar{z} = 7$ and $\bar{z} = 21$), the radius of the artery is $\bar{R}_0\, a(\bar{t})$ which is the radius of the normal artery and at the throat of the stenosis, the radius of the artery is minimum with the value of $(\bar{R}_0 - \bar{\delta})a(\bar{t})$. Further, we have taken the length of the arterial segment as 14 units in the axial direction with $\bar{z}_0 = 7$ (semi-length of the stenosis) $\bar{z}_1 = 14$ (centre position of the stenosis) and the arterial stenosis is assumed to be present between $\bar{z} = 7$ and $\bar{z} = 21$ in the axial direction. We assumed that the stenosis depth is also dependent on time, we have taken the arterial radius $\bar{R}(\bar{z},\bar{t})$ as the product of function of axial distance $\bar{R}_0 - (\bar{\delta}/2)\left(1+\cos\left[\pi(\bar{z}-\bar{z}_1)/\bar{z}_0\right]\right)$ and the time dependent function $a(\bar{t})$.

Consider an axially symmetric, laminar, unsteady (pulsatile) and fully developed flow of a non-Newtonian incompressible viscous electrically conducting fluid in the axial direction $(\bar{z})$ through a circular artery with an axisymmetric mild stenosis in the presence of uniform transverse magnetic field (B_0). The non-Newtonian rheology of the flowing blood is characterized by the Casson fluid model. The wall of the artery is assumed to be rigid (because of the presence of the stenosis) and the artery is assumed to be too long so that the entrance and end effects can be neglected in the arterial segment under study. The equations of continuity and momentum governing the magnetohydrodynamic (MHD) flow are [10]

$$\nabla \bullet \mathbf{V} = 0$$

(3)

$$\frac{D\mathbf{V}}{Dt} = -\frac{1}{\rho}\nabla\bar{p} + \nabla \bullet \tau + \mathbf{J}$$

(4)

where $\bar{\rho}$ is the density of blood, $\mathbf{V}$ is the velocity vector, $D\mathbf{V}/Dt$ is the material derivative, $\bar{p}$ is the pressure, $\boldsymbol{\tau}$ is the stress tensor, $\mathbf{J}$ is the current density, $\mathbf{B} = \mathbf{B_0} + \mathbf{B_1}$ is the total magnetic field, $\mathbf{B_1}$ is the induced magnetic field assumed to be negligibly small in comparison with the external magnetic field B_0 for MHD flow at small magnetic Reynolds number. We assume that the electric field due to the polarization of charge is also negligible. By Ohm's law, we have [10]

$$\mathbf{J} = \sigma\left(\mathbf{E} + \mathbf{V} \times \mathbf{B}\right)$$

(5)

where σ is the electrical conductivity and E is the electric field. The imposed and induced electrical fields are assumed to be negligible. Thus, the term $\mathbf{J} \times \mathbf{B}$ can be simplified as [19]

$$\mathbf{J} \times \mathbf{B} = -\sigma \mathbf{B}^2 \mathbf{V}. \tag{6}$$

It can be shown that the radial velocity is negligibly small and can be neglected for a low Reynolds number flow. Thus, the momentum equations in the $\bar{r}$ and $\bar{z}$ directions in the presence of MHD interactions simplifies to

$$0 = -\frac{\partial \bar{p}}{\partial \bar{r}} \tag{7}$$

$$\bar{\rho}\frac{\partial \bar{u}}{\partial \bar{t}} = -\frac{\partial \bar{p}}{\partial \bar{z}} - \frac{1}{\bar{r}}\frac{\partial}{\partial \bar{r}}(\bar{r}\,\bar{\tau}) - \sigma B_0^2 \bar{u} \tag{8}$$

where $\bar{\tau} = \bar{\tau}_{rz}$ is the shear stress. The constitutive equation of the Casson fluid model which represents the blood is [27-29]

$$-\frac{\partial \bar{u}}{\partial \bar{r}} = \begin{cases} \dfrac{1}{\bar{\mu}_C}\left(\sqrt{\bar{\tau}} - \sqrt{\bar{\tau}_C}\right)^2 & \text{if } \bar{\tau} \geq \bar{\tau}_C \\ 0 & \text{otherwise} \end{cases} \tag{9}$$

where $\bar{\mu}_C$ and $\bar{\tau}_C$ are the viscosity and yield stress of the Casson fluid respectively. Eq. (9) emphasizes that normal flow occurs whenever the shear stress is greater than the yield stress and plug flow occurs in the other case. Resolving Eq. (9) for the shear stress $\bar{\tau}$ and then substituting it in Eq. (8), one can get

$$\frac{\partial \bar{u}}{\partial \bar{t}} = -\frac{1}{\bar{\rho}}\frac{\partial \bar{p}}{\partial \bar{z}} - \frac{\bar{\mu}_C}{\bar{\rho}\bar{r}}\frac{\partial}{\partial \bar{r}}\left[\bar{r}\left\{\left(-\frac{\partial \bar{u}}{\partial \bar{r}}\right) + \frac{\bar{\tau}_C}{\bar{\mu}_C} + 2\sqrt{\frac{\bar{\tau}_C}{\bar{\mu}_C}\left(-\frac{\partial \bar{u}}{\partial \bar{r}}\right)}\right\}\right] - \frac{\sigma B_0^2 \bar{u}}{\bar{\rho}}. \tag{10}$$

$(\partial \bar{p}/\partial \bar{z})$ is the pressure gradient which is due to the pumping action of the heart and for pulsatile flow and is taken as

$$-\frac{\partial \bar{p}}{\partial \bar{z}} = \bar{A}_0 + \bar{A}_1 \cos \bar{\omega} \bar{t} \tag{11}$$

where $\bar{A}_0$ and $\bar{A}_1$ are the amplitude of the constant pressure gradient and pulsatile pressure gradient and $\bar{\omega} = 2\pi \bar{f}$, $\bar{f}$ is the heart pulse rate.

2.2 Non-dimensionalization

Let us introduce the following non-dimensional variables.

$$r = \frac{\bar{r}}{\bar{R}_0}, \ z = \frac{\bar{z}}{\bar{R}_0}, \ u = \frac{\bar{u}}{\bar{U}}, \ t = \frac{\bar{t}\,\bar{U}}{\bar{R}_0}, \ p = \frac{\bar{p}}{\bar{\rho}\bar{U}^2}, \ \omega = \frac{\bar{\omega}\bar{R}_0}{\bar{U}},$$

$$A_0 = \frac{\bar{R}_0 \bar{A}_0}{\bar{\rho}\bar{U}^2}, \ A_1 = \frac{\bar{R}_0 \bar{A}_1}{\bar{\rho}\bar{U}^2}, \ \delta = \frac{\bar{\delta}}{\bar{R}_0}, \ \theta = \frac{\bar{\tau}_C}{(\bar{\mu}_C \bar{U}/\bar{R}_0)}. \tag{12}$$

Applying the non-dimensional variables (12) into Eqs. (1), (2), (10) and (11), one can obtain

$$R(z,t) = \begin{cases} \left[1 - \dfrac{\delta}{2}\left(1 + \cos\left[\pi(z - z_1)/z_0\right]\right)\right]a(t) & \text{if } d \leq z \leq d + 2z_0 \\ a(t) & \text{in the non-stenotic region} \end{cases} \tag{13}$$

$$a(t) = 1 - k\cos(\omega t - \phi) \tag{14}$$

$$\frac{\partial u}{\partial t} = -\frac{\partial p}{\partial z} - \frac{1}{Re}\frac{1}{r}\frac{\partial}{\partial r}\left[r\left(-\frac{\partial u}{\partial r}\right) + \theta + 2\sqrt{\theta\left(-\frac{\partial u}{\partial r}\right)}\right] - \frac{H^2 u}{Re} \tag{15}$$

$$-\frac{\partial p}{\partial z} = A_0 + A_1 \cos \omega t \tag{16}$$

where $Re = \left(\bar{\rho}\bar{R}_0\bar{U}\right)/\bar{\mu}_C$ is the pulsatile Reynolds and $H = \left[\left(B_0 \bar{R}_0 \sqrt{\sigma}\right)/\sqrt{\bar{\mu}_C}\right]$ is the Hartmann number. The non-dimensional form of the appropriate boundary and initial conditions are [8, 10]

$$\frac{\partial u}{\partial r}(0,z,t) = 0; \quad u(0,z,t) = 0 \quad \text{at } r = R \tag{17, 18}$$

$$u(r,z,0) = \begin{cases} \left(\dfrac{A_0 + A_1}{H^2}\right)\left\{1 - \dfrac{I_0(Hr)}{I_0(H)}\right\} & \begin{array}{l}\text{in the presence}\\ \text{of magnetic field}\end{array} \\ \left(\dfrac{A_0 + A_1}{4}\right)\left(1 - r^2\right) & \begin{array}{l}\text{in the absence of}\\ \text{magnetic field.}\end{array} \end{cases} \tag{19}$$

2.3 Radial coordinate transformation

Applying the radial coordinate transformation $\xi = r/R(z,t)$ into the momentum Eq. (15) and boundary and initial conditions (17)-(19), one can obtain

$$\frac{\partial u}{\partial t} = -\frac{\partial p}{\partial z} - \frac{1}{Re}\left[\frac{1}{R^2\xi^2}\left(-\frac{\partial u}{\partial \xi}\right) + \frac{\theta}{R\xi^2} + \frac{2}{\xi^2}\sqrt{\frac{\theta}{R^3}\left(-\frac{\partial u}{\partial \xi}\right)}\right.$$
$$\left. + \frac{1}{R^2\xi}\left(-\frac{\partial^2 u}{\partial \xi^2}\right) - \frac{1}{\xi}\sqrt{\frac{\theta}{R^3}\left(-\frac{\partial u}{\partial \xi}\right)^{-1}}\left(-\frac{\partial^2 u}{\partial \xi^2}\right) + H^2 u\right]. \tag{20}$$

The appropriate boundary and initial conditions are

$$\frac{\partial u}{\partial \xi}(0,z,t) = 0, \ u(1,z,t) = 0 \tag{21, 22}$$

$$u(\xi,z,0) = \begin{cases} \left(\dfrac{A_0 + A_1}{H^2}\right)\left\{1 - \dfrac{I_0(H\xi R)}{I_0(H)}\right\} & \begin{array}{l}\text{in the presence}\\ \text{of magnetic field}\end{array} \\ \left(\dfrac{A_0 + A_1}{4}\right)\left(1 - (R\xi)^2\right) & \begin{array}{l}\text{in the presence}\\ \text{of magnetic field.}\end{array} \end{cases} \tag{23}$$

3. Finite difference method of solution

Though many computational methods are available to solve the nonlinear partial differential equation, Eq. (20), with the boundary and initial conditions (21)-(23), finite difference method is a more easy and efficient method for solving such nonlinear partial differential equations. Forward difference formula is used to express the time derivative and central dif-

ference formula is applied to the spatial derivatives and is given below:

$$\frac{\partial u}{\partial t} = \frac{(u)_{i,j}^{k+1} - (u)_{i,j}^{k}}{\Delta t} \tag{24}$$

$$\frac{\partial u}{\partial \xi} = \frac{(u)_{i,j+1}^{k} - (u)_{i,j-1}^{k}}{2\Delta \xi} = \left(u_{f\xi}\right)_{i,j}^{k} \tag{25}$$

$$\frac{\partial^2 u}{\partial \xi^2} = \frac{(u)_{i,j+1}^{k} - 2(u)_{i,j}^{k} + (u)_{i,j-1}^{k}}{(\Delta x)^2} = \left(u_{sx}\right)_{i,j}^{k} \tag{26}$$

where $\xi_j = (j-1)\Delta\xi$, $j = 1,2,.....N+1$ such that $\xi_{N+1} = 1$; $z_j = (i-1)\Delta z$, $i = 1,2,....M+1$; $t_k = (k-1)\Delta t$, $k = 1,2,....$ for the entire arterial segment under consideration with $\Delta\xi$ and Δz as the respective increments in the radial and axial directions and Δt is the time increment. On using Eqs. (24)-(26), the simplified momentum equation, Eq. (20) transformed into the following finite difference equation for the velocity field:

$$u_{i,j}^{k+1} = u_{i,j}^{k} + \Delta t \left[-\left(\frac{\partial p}{\partial z}\right)^{k+1} - \frac{1}{Re}\left\{ \frac{1}{\left(R_i^k \xi_j\right)^2}\left\{ -\left(u_{f\xi}\right)_{i,j}^{k} \right\} \right. \right.$$
$$+ \frac{1}{\left(R_i^k\right)^2 \xi_j}\left\{ -\left(u_{s\xi}\right)_{i,j}^{k} \right\} + \frac{\theta}{R_i^k \xi_j^2} + \frac{2}{\xi_j^2}\sqrt{\frac{\theta}{\left(R_i^k\right)^3}}\left\{ -\left(u_{f\xi}\right)_{i,j}^{k} \right\}$$
$$\left. \left. - \frac{1}{\xi_j}\sqrt{\frac{\theta}{\left(R_i^k\right)^3}\left\{ -\left(u_{f\xi}\right)_{i,j}^{k} \right\}^{-1}\left\{ -\left(u_{s\xi}\right)_{i,j}^{k} \right\}} + H^2 u_{i,j}^{k} \right\} \right]. \tag{27}$$

Using Eqs. (24)-(26) in Eqs. (21)-(23), one can obtain the following difference equations as the boundary and initial conditions.

$$u_{i,1}^{k} = u_{i,2}^{k}; \qquad u_{i,N+1}^{k} = 0 \tag{28, 29}$$

$$u_{i,j}^{1} = \begin{cases} \left(\frac{A_0 + A_1}{H^2}\right)\left\{1 - \frac{I_0\left(H\xi_j R_i^1\right)}{H^2}\right\} & \text{in the presence of magnetic field} \\ \left(\frac{A_0 + A_1}{4}\right)\left(1 - \left(\xi_j R_i^1\right)^2\right) & \text{in the presence of magnetic field} \end{cases} \tag{30}$$

After computing the velocity distribution in the flow domain, one can compute the flow rate, wall shear stress and longitudinal impedance respectively using the following formulas.

$$Q_i^k = 2\pi\left(R_i^k\right)^2\left[\int_0^\beta \xi_j u_{i,j}^k \, d\xi_j + \int_\beta^1 \xi_j u_{i,j}^k \, d\xi_j\right] \tag{31}$$

$$\left(\tau_w\right)_i^k = \theta + \frac{1}{R_i^k}\left\{ -\left(u_{f\xi}\right)_{i,N}^k \right\} + 2\sqrt{\frac{\theta}{R_i^k}\left\{ -\left(u_{f\xi}\right)_{i,N}^k \right\}} \tag{32}$$

$$\Lambda_i^k = \left(-\frac{\partial p}{\partial z}\right)^k \Big/ Q_i^k \tag{33}$$

where β is the plug core radius. For a better understanding of the present study, all the important steps of this research problem are given below in the form of a flow chart.
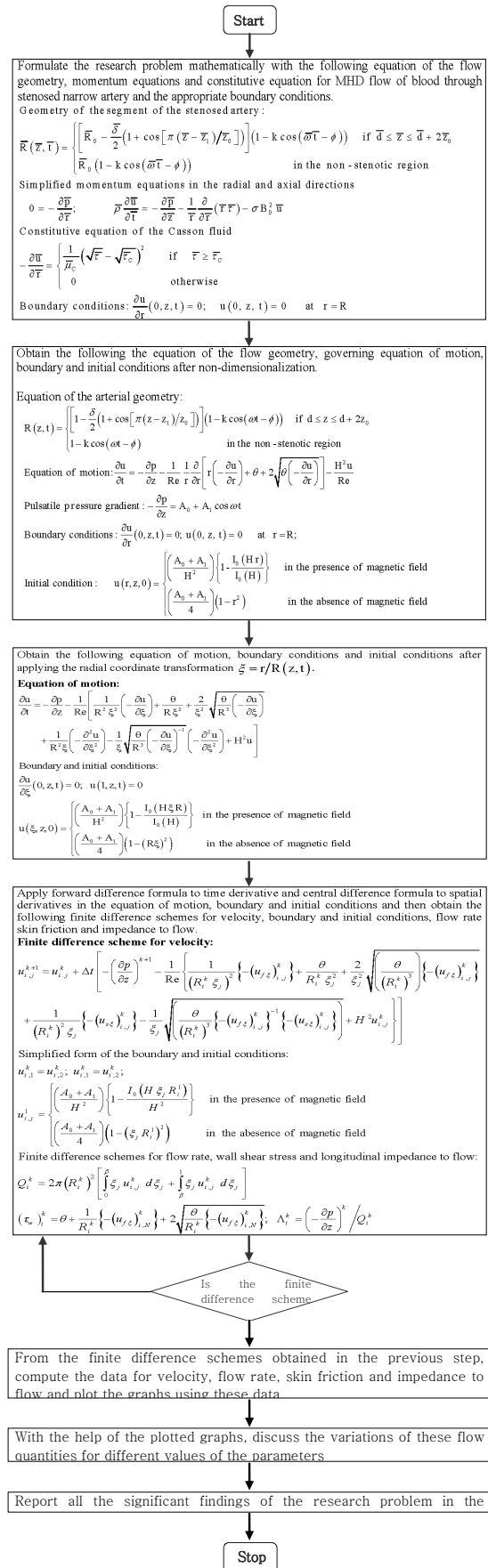
4. Numerical simulations of results and discussion

The aim of this study is to understand and bring out the effects of the magnetic field, pressure gradient, phase angle, yield stress and stenosis height on the velocity, flow rate, wall shear stress and longitudinal impedance to flow in blood flow through a stenosed artery when the flowing blood is modeled as Casson fluid model. For the numerical simulation of the various flow quantities and to validate the present results with the existing results, we have used the following parameter values (range) [10].

$$d = z_0 = 7, z_1 = 14, \ Re = 300, \ A_0 = 0.2 A_1, \ \beta = 0.025$$
$$A_0 : 0.2 - 0.8; \ k, \omega : 0.02 - 0.05; \ \phi : 0.2 - 0.5, \ H : 0 - 4; \theta :$$
$$0 - 0.15; \ \delta : 0 - 0.25, t : 0 - 90$$

The explicit finite difference scheme is found to be effective in solving the partial differential equations numerically. We have chosen the time step as $\Delta t = 0.0001$ for convergent of the solution to the fifth order. The flow region is discretized by taking the step size in the axial direction and radial direction respectively as $\Delta z = 0.05$ and $\Delta \xi = 0.025$. Programming codes are developed to compute the data for the flow quantities velocity, flow rate, skin friction and longitudinal impedance to flow, using standard programming languages.

4.1 Velocity distribution

The velocity profiles are of particular interest, since, they provide a detailed description of the flow field. The velocity distribution for different values of the Hartmann number H (parameter of the magnetic field) with $A_0 = 0.2$, $\omega = k = 0.02$, $\phi = 0.2$, $\theta = 0.1$, $\delta = 0.276$, $z = 14$ and $t = 50$ is depicted in Fig. 2. It is observed that the velocity decreases significantly with the increase of the Hartmann number H. It means that the presence of the magnetic field influences the velocity field by decreasing its magnitude. Although the velocity distribution of the Newtonian fluid model in the present study shows a slightly lower magnitude than that of the Newtonian fluid model in Fig. 2 of Ikbal et al. [10], this difference is not very significant and so the results of the present study can be considered to be very closely in agreement with the established results of Ikbal et al. [10].

Fig. 3 shows the velocity distribution at discrete points in the axial direction (since, the stenosis is assumed to be symmetric, we have taken the discrete points in the first half of the stenosis) with $A_0 = 0.2$, $\omega = k = 0.02$, $\phi = 0.2$, $\theta = 0.1$, $H = 2$, $\delta = 0.1$ and $t = 50$. It is noted that the velocity increases marginally with the increase of the axial variable z in the first half of the stenosis and this behavior is reversed in the second half of the stenosis (not shown in the figure). Figs. 2 and 3 bring out the effects of magnetic filed and yield stress on the velocity distribution of the blood when it flows through stenosed arteries.
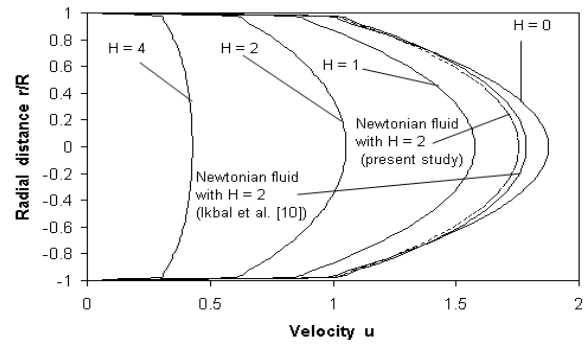

Fig. 2. Velocity distribution for different values of Hartmann number with $A_0 = \phi = 0.2$, $\omega = k = 0.02$, $\theta = 0.1$, $\delta = 0.276$, $z = 14$ and $t = 50$.
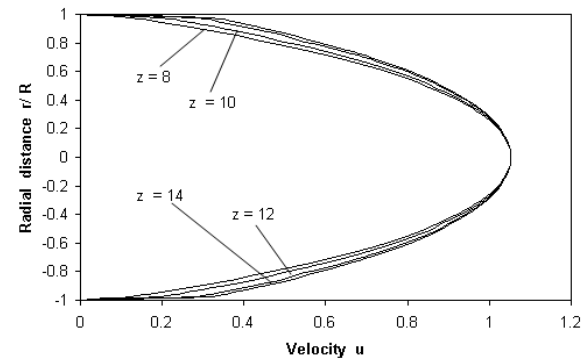

Fig. 3. Velocity distribution at discrete axial points with $A_0 = 0.2$, $\omega = k = 0.02$, $\phi = 0.2$, $\theta = 0.1$, $H = 2$, $\delta = 0.1$ and $t = 50$.

4.2 Flow rate

Fig. 4 illustrates the variation of flow rate with constant amplitude (A_0) of the pressure gradient for different values of the Hartmann number H with $\omega = k = 0.02$, $\phi = 0.2$, $\theta = 0.1$, $\delta = 0.1$, $z = 14$ and $t = 50$. It is clear that the flow rate increases linearly with the increase of the pressure gradient of the blood flow. It is also noticed that the flow rate decreases significantly with the increase of the Hartmann number H, i.e. the presence of the magnetic field also influences the flow rate by reducing its magnitude very significantly. The variation of flow rate with time for different values of the amplitude parameter k of the artery radius and phase angle ϕ with $A_0 = 0.5$, $\omega = 0.02$, $\theta = 0.1$, $\delta = 0.1$ and $z = 14$ is sketched in Fig. 5. It is noticed that the flow rate decreases gradually (linearly) with the increase of the time t from 0 to 80 and then it decreases considerably as t increases further from 80 to 90. For a given value of the phase angle ϕ, the flow rate increases marginally with the increase of the amplitude parameter k of the artery radius. It is further observed that the flow rate decreases slightly with the increase of the phase angle ϕ when the amplitude parameter k is kept as constant. Figs. 4 and 5 show the effects of magnetic field, pressure gradient, phase angle and amplitude of the artery radius on the flow rate of blood in stenosed arteries.
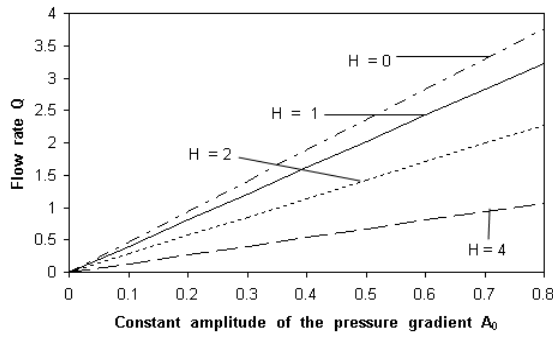
Fig. 4. Variation of flow rate with constant amplitude of the pressure gradient for different values of the Hartmann number with $\omega = k = 0.02$, $\phi = 0.2$, $\theta = 0.1$, $\delta = 0.1$, $z = 14$ and $t = 50$.

Fig. 5. Variation of flow rate with time for different values of the Hartmann number with $A_0 = 0.5$, $\omega = 0.02$, $\theta = 0.1$, $\delta = 0.1$ and $z = 14$.
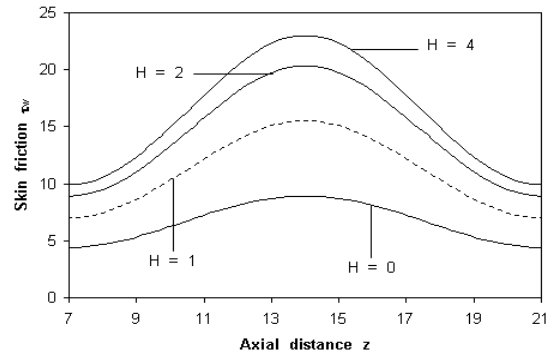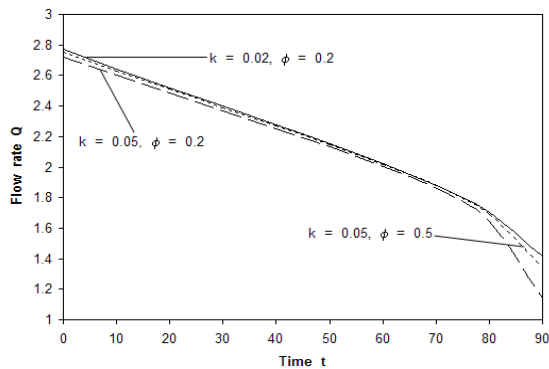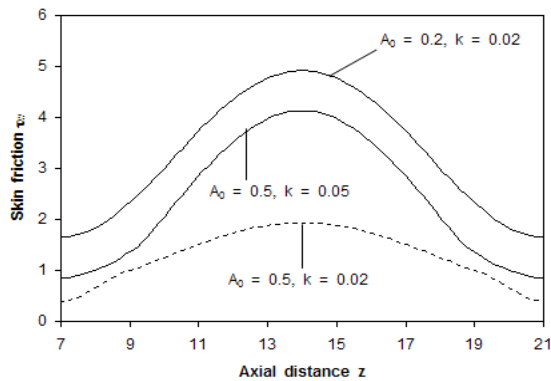

Fig. 6. Variation of skin friction with axial distance for different values of the Hartmann number with $A_0 = 0.5$, $\omega = 0.02$, $\theta = \delta = 0.1$ and $z = 14$.

Fig. 7. Variation of skin friction with axial distance for different values of A and k with $\omega = 0.02$, $\phi = 0.2$, $H = 2$, $\theta = \delta = 0.1$ and $t = 50$.
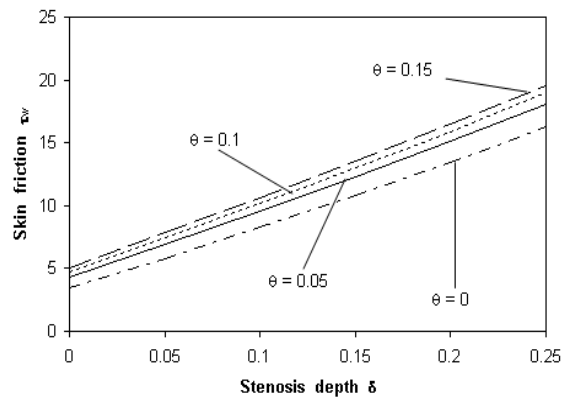

Fig. 8. Variation of skin friction with stenosis depth for different values of yield stress with $\omega = k = 0.02$, $\phi = 0.2$, $H = 2$, $A_0 = 0.5$, $z = 14$ and $t = 50$.

4.3 Skin friction

Skin friction is an important parameter in the studies of the blood flow through arterial stenosis. Accurate predictions of skin friction distributions are particularly useful in the understanding of the effects of blood flow on the endothelial cells [33-35]. Fig. 6 shows the variation of skin friction with axial distance for different values of the Hartmann number H with $A_0 = 0.5$, $\omega = 0.02$, $\theta = 0.1$, $\delta = 0.1$ and $z = 14$. One can note that the skin friction increases with the increase of the axial variable from 7 to 14 and then it decreases symmetrically as the axial variable z increases further from 14 to 21. It is seen that the skin friction increases significantly with the increase of the Hartmann number H which indicates that the presence of magnetic field also affects the blood flow by increasing the skin friction.

The variation of skin friction with axial distance for different values of A_0 and k with $\delta = 0.1$, $\omega = 0.02$, $\phi = 0.2$, $H = 2$, $\theta = 0.1$, and $t = 50$ is depicted in Fig. 7. It is clear that for a given value of k, the skin friction decreases considerably with the increase of the pressure gradient parameter A_0. This behavior is reversed when the amplitude parameter k of the artery radius increases while the pressure gradient parameter A_0 is fixed. Fig. 8 shows the variation of skin friction with stenosis depth for different values of yield stress θ with $\phi = 0.2$, $\omega =$

0.02, $H = 2$, $A_0 = 0.5$, $k = 0.02$, $z = 14$ and $t = 50$. It is noticed that the skin friction increases slightly nonlinearly with the increase of the stenosis depth δ. It is also found that the skin friction increases marginally with the increase of the yield stress θ. Figs. 6-8 spell out the effects of magnetic field, pressure gradient, yield stress and stenosis depth on the skin friction of blood flow.

Table 1. Estimates of the increase in skin friction due to the presence of magnetic field at discrete points in the axial direction with $A_0 = 0.7$, $Re = 300$, $k = \omega = 0.02$, $t = 50$, $\theta = \delta = 0.1$ and $\phi = 0.2$.

H \ Z	7	8	9	10	11	12	13	14
1	1.5937	1.6020	1.6244	1.6548	1.6868	1.7143	1.7329	1.7395
2	2.0202	2.0359	2.0748	2.1289	2.1860	2.2357	2.2693	2.2811
4	2.2526	2.2709	2.3204	2.3879	2.4591	2.5211	2.5632	2.5780

Table 2. Estimates of the increase in longitudinal impedance due to the presence of magnetic field at discrete points in the axial direction with $A_0 = 0.7$, $Re = 300$, $k = \omega = 0.02$, $\theta = \delta = 0.1$ and $\phi = 0.2$.

H \ Z	7	8	9	10	11	12	13	14
1	1.1659	1.1660	1.1662	1.1666	1.1671	1.1675	1.1679	1.1681
2	1.6554	1.6556	1.6566	1.6584	1.6609	1.6635	1.6654	1.6662
4	3.5259	3.5278	3.5359	3.5476	3.5649	3.5828	3.5963	3.6021

4.4 Longitudinal impedance

The variation of the longitudinal impedance to blood flow with stenosis depth for different values of the Hartmann number H and the amplitude parameter k of the artery radius with $\omega = 0.02$, $\phi = 0.2$, $A_0 = 0.5$, $\delta = 0.1$, $z = 14$ and $t = 50$ is illustrated in Fig. 9. One can note that the longitudinal impedance to the flow increases almost linearly with the increase of the stenosis depth δ for lower values of the Hartmann number ($H = 0, 2$) and increases nonlinearly with the stenosis depth δ for higher value of the Hartmann number ($H = 4$). It is observed that for a given value of the amplitude parameter k of the artery radius, the longitudinal impedance increases significantly. It is also found that the longitudinal impedance increases marginally with the increase of the amplitude parameter k of the artery radius when the Hartmann number is held constant. Fig. 9 brings out the effects of the magnetic field, stenosis depth and radius of the artery on the longitudinal impedance of the blood flow.

4.5 Quantification of skin friction and longitudinal impedance

The increase in skin friction and longitudinal impedance to flow due to the presence of the magnetic field is treated as an important measure in Hemodynamics which is useful to understand the effect of the magnetic field. The increase in the skin friction/longitudinal impedance due to the presence of the magnetic field is defined as the ratio between the skin friction/longitudinal impedance of a fluid model in the presence of magnetic field for a given set of values of the parameters and the skin friction/longitudinal impedance of the same fluid in the absence of the magnetic field for the same set of values of the parameters. The estimates of the increase in the skin friction for different values of the magnetic field parameter H in the axial direction (upto the half of the stenosis length) with $A_0 = 0.7$, $Re = 300$, $k = \omega = 0.02$, $t = 50$, $\theta = \delta = 0.1$ and $\phi = 0.2$ are computed in Table 1. It is observed that estimates of
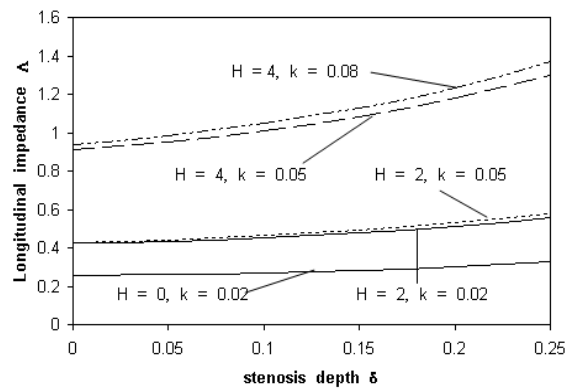

Fig. 9. Variation of longitudinal impedance with stenosis depth for different values of H and k with $\omega = 0.02$, $\phi = 0.2$, $A_0 = 0.5$, $\theta = 0.1$, $z = 14$ and $t = 50$.

the increase in the skin friction increases slightly with the increase of the axial variable 'z' and it increases considerably with the increase of the Hartmann number H. The estimates of the increase in longitudinal impedance for different values of the Hartmann number H in the axial direction with $A_0 = 0.7$, $Re = 300$, $k = \omega = 0.02$, $t = 50$, $\theta = \delta = 0.1$ and $\phi = 0.2$ are given in Table 2. It is noticed that the estimates of the increase in the longitudinal impedance increases significantly with the increase of the Hartmann number H and it increases very slightly with the increase of the axial variable 'z'. It is of interest to note that the presence of magnetic field influences the magnitude of the skin friction and longitudinal impedance of the flow by increasing their magnitude considerably.

5. Conclusion

The present study analyzes the pulsatile flow of Casson fluid model for blood flow through stenosed arteries in the presence of the magnetic field and brings out some interesting results. The results point out the following features:
(i) The velocity and flow rate decrease and the skin friction

and longitudinal impedance to the flow increase considerably with the increase of the magnetic field parameter. On the other hand, the flow rate increases and skin friction decreases with the increase of the pressure gradient.

(ii) The skin friction and longitudinal impedance to flow increases with the increase of the stenosis depth, whereas the flow rate decreases and skin friction and longitudinal impedance increase with the increase of the amplitude parameter of the artery radius.

(iii) The estimates of the increase in the skin friction and longitudinal impedance to flow increase considerably with the increase of the intensity of the magnetic field.

(iv) Thus the contribution in the present study is useful to predict the physiologically important flow quantities which may find applications in the clinical studies.

Acknowledgement

Nomenclature━━━━━━━━━━━━━━━

$\bar{r}$	: Radial coordinate
$\bar{z}$	: Axial coordinate
$\bar{z}_0$	: Semi-length of the stenosis
z_1	: Centre of the stenosis
B_0	: Uniform transverse magnetic field parameter
$\bar{R}$	: Radius of the arterial segment
$\bar{R}_0$	: Radius of the normal artery
a	: Time dependent function of the stenosis depth
k	: Amplitude parameter of the stenosis depth
$\bar{f}$	: Heart pulse frequency
$\mathbf{V}$	: Velocity vector
$\bar{p}$	: Pressure
$\mathbf{B}_1$	: Induced magnetic field parameter
$\mathbf{J}$	: Current density
$\bar{A}_0$	: Constant pressure gradient
$\bar{A}_1$	: Pulsatile pressure gradient
$\bar{u}$	: Axial component of velocity
Re	: Reynolds number
H	: Hartmann number
$\bar{U}$	: Characteristic velocity
$\bar{d}$	: Starting point of the stenosis

Greek symbols

$\bar{\psi}$	: Azimuthal angle
ξ	: Radial coordinate transformation
θ	: Yield stress in non-dimensional form
β	: Plug core radius
ϕ	: Phase angle
$\Delta\xi$	: Increment in the radial direction

$\bar{\mu}_c$	: Viscosity of Casson fluid
σ	: Electrical conductivity
τ	: Stress tensor
$\bar{\tau}$	: Shear stress
$\bar{\tau}_c$	: Yield stress
$\bar{\delta}$	: Maximum projection of the stenosis
$\bar{\rho}$	: Density of blood
$\bar{\omega}$	: Angular frequency
Δz	: Increment in the axial direction
Δt	: Increment in time scale

References

[1] H. A. Hogan and M. Henriksen, An evaluation of a micropolar model for blood flow through an idealized stenosis, *J. Biomech.,* 22 (3) (1989) 21-218.

[2] M. D. Deshpande, D. P. Giddens and R. F. Mabon, Steady laminar flow through modeled vascular stenoses, *J. Biomech.*, 9 (1976) 165-174.

[3] I. Marshall, S. Zhao, P. Papathanasopoulou, P. Hoskins and X. Y. Xu, MRI and CFD studies of pulsatile flow in healthy and stenosed carotid bifurcation models, *J. Biomech.,* 27 (2004) 679- 687.

[4] E. W. Merrill, A. M. Benis, E. R. Gilliland, T. K. Sherwood and E. W. Salzman, Pressure flow relations of human blood in hallow fibers at low shear rates, *J. Appl. Physiol.*, 20 (1965) 954- 967.

[5] A. P. Dwivedi, T. S. Pal and L. Rakesh, Micropolar fluid model for blood flow through small tapered tube, *Indian J. Technology,* 20 (1982) 295-299.

[6] C. Tu and M. Deville, Pulsatile flow of non-Newtonian fluids through arterial stenosis, *J. Biomech.,* 29 (1996) 899-908.

[7] M. Motta, Y. Haik, A. Gandhari and C. J. Chen, High magnetic field effects on human deoxygenated hemoglobin light absorption, *Bioelectrochem. Bioenerg.,* 47 (1998) 297-300.

[8] E. F. EL-Shehawey, E. M. E. Elbarbary, N. A. S. Afifi and M. Elshahed, MHD flow of an elastico-viscous fluid under periodic body acceleration, *J. Math. & Math. Sci.,* 23 (2000) 795-799.

[9] C. Midya, G. C. Layek, A. S. Gupta and T. Roy Mahapatra, Magenetohydrodynamic viscous flow separation in a channel with constrictions, *ASME. J. Fluid Eng.,* 125 (2003) 952-962.

[10] Md. A. Ikbal, S. Chakravarty, K. L. Kelvin Wong, J. Mazumdar and P. K. Mandal, Unsteady response of non-Newtonian blood flow through a stenosed artery in magnetic field, *J. Computat. Appl. Math.,* 230 (2009) 243-259.

[11] A. Ramachandra Rao and K. S. Deshikachar, Physiological type flow in a circular pipe in the presence of a transverse magnetic field, *J. Indian Inst. Sci.,* 68 (1988) 247-260.

[12] P. A. Voltairas, D. I. Fotiadis and L. K. Michalis, Hydrodynamics of magnetic drug targeting, *J. Biomech.,* 35 (2002) 813-821.

[13] V. A. Vardayan, Effect of magnetic field on blood flow, *Biotizaka,* 18 (1973) 494- 496.

[14] R. Bhargava, S. Rawat, H. S. Takhar and O. A. Beg, Pulsatile magneto-biofluid flow and mass transfer in a non-Darcian porous medium channel, *Meccanica,* 42 (2007) 247-262.

[15] K. Haldar and S. N. Ghosh, Effect of a magnetic field on blood flow through an indented tube in the presence of erythrocytes, *Indian J. Pure. Appli. Math.*, 25 (1994) 345-352.

[16] Y. Haik, V. Pai and C. J. Chen, Apparent viscosity of human blood in a high static magnetic field, *J. Magn. Magn. Mater.,* 225 (2001) 180-186.

[17] E. Amos and A. Ogulu, Magentic effect on pulsatile flow in a constricted axis-symmetric tube, *Indian J. Pure Appl. Math.,* 34 (9) (2003) 1315-1326.

[18] E. E. Tzirtzilakis, A mathematical model for blood flow in magnetic field, *Phys. Fluids,* 17 (2005) 077103- 077115.

[19] R. Bali and U. Awasthi, Effect of a magnetic field on the resistance to blood flow through stenotic artery, *Appl. Math. Computat.,* 188 (2007) 1635- 1641.

[20] W. L. Siauw, E. Y. K. Ng and J. Mazumdar, Unsteady stenosis flow prediction: a comparitve study of non-Newtonian models with operator splitting scheme, *Med. Eng. Phys.,* 22 (2000) 265-277.

[21] P. K. Mandal, S. Chakravarty, A. Mandal and N. Amin, Effect of body acceleration on unsteady generalized pulsatile flow of non-Newtonian fluid through a stenosed artery, *Appl. Math. Computat.,* 189 (2007) 766-799.

[22] D. S. Sankar and Usik Lee, Two-phase non-linear model for the flow through stenosed blood vessels, *J. Mech. Sci. Tech.,* 21 (2007) 678-689.

[23] J. C. Misra, B. Pal and A. S. Gupta, Hydromagnetic flow of a second-grade fluid in a channel – Some applications to physiological Systems, *Math. Models Methods Appl. Sci.,* 8 (1998) 1323-1342.

[24] R. Bhargava, Sugandha, H. S. Takhar and O. A. Beg, Computational simulation of biomagnetic micropolar blood flow in porous media, *J. Biomech.,* 39 (2006) S648-S649.

[25] O. A. Beg, H. S. Takhar, R. Bhargava, S. Sharma and T. K. Hung, Mathematical modeling of biomagnetic flow in a micropolar fluid-saturated Darcian porous medium, *Int. J. Fluid Mech. Res.,* 34 (2007) 403- 424.

[26] H. A. Attia and M. E. S. Ahmed, Unsteady hydromagnetic generalized Couette flow of a non-Newtonian fluid with heat transfer between parallel porous plates, *Journal of heat transfer,* 130 (2008) 114504 – 1-5.

[27] N. Casson, In: Rheology of disperse systems (Edited by Mill, C. C). Pergamon Press, London, 1959.

[28] G. W. Scott Blair, An equation for the flow of blood, Plasma and Serum through Glass Capillaries, *Nature,* 183 (1959) 613.

[29] A. L. Copley, In: Flow properties of blood and other biological systems (Edited by Copley, A. L., Stainsby, G) Pergamon Press, Oxford, 1960.

[30] E. W. Merrill, A. M. Benis, E. R. Gilliland, T. K. Sherwood, E. W. Salzman, Pressure flow relations of human blood in hollow fibers at low shear rates, *J. Appl. Physiol.,* 20 (1965) 954.

[31] S. E. Charm and G. Kurland, Viscometry of human blood for shear rates of 0 – 100,000 sec^{-1}, *Nature,* 206 (1965) 617.

[32] G. W. Scott Blair and D. C. Spanner, An introduction to Biorheology, Elsevier, Amsterdam, Oxford and New York, 1974.

[33] J. J. Chiu, D. L. Wang, S. Chien, R. Skalak and S. Usami S. Effects of disturbed flow on endothelial cells, *J. Biomech. Eng.,* 120 (1998) 2-8.

[34] G. G. Galbraith, R. Skalak and S. Chien S, Shear stress induces spatial reorganization of the endothelial cell cytoskeleton, *Cell Motility and the Cytoskeleton,* 40 (1988) 317-330.

[35] T. Karino and H. L. Goldsmith, Flow behavior of blood cells and rigid spheres in annular vortex, *Philosophical Transactions Royal Society,* London 1977; B279: 413- 445.

D. S. Sankar received his B. Sc degree in Mathematics from the University of Madras, India, in 1989. He then received his M. Sc., M. Phil. And Ph.D degrees from Anna University, India, in 1991, 1992 and 2004 respectively. Dr. D. S. Sankar is currently an Associate Professor in the School of Mathematical Sciences, Universiti Sains Malaysia, Malaysia. His serves as a referee for several reputed ISI journals and his research interest includes fluid dynamics, hemodynamics, differential equations and numerical analysis.

Usik Lee received his B.S. degree in Mechanical Engineering from Yonsei University, Korea in 1979. He then received his M.S. and Ph.D degrees in Mechanical Engineering from Stanford University, USA in 1982 and 1985, respectively. Dr. Lee is currently a Professor at the Department of Mechanical Engineering at Inha University in Incheon, Korea. He has served as a referee for many reputed international journals. Dr. Lee's research interests include structural dynamics, biomechanics, and computational mechanics.